J Sol-Gel Sci Technol (2015) 73:434–442
DOI 10.1007/s10971-014-3555-6

ORIGINAL PAPER

Novel sol–gel preparation of $(P_2O_5)_{0.4}$–$(CaO)_{0.25}$–$(Na_2O)_X$–$(TiO_2)_{(0.35–X)}$ bioresorbable glasses (X = 0.05, 0.1, and 0.15)

Farzad Foroutan · Nora H. de Leeuw · Richard A. Martin · Graham Palmer · Gareth J. Owens · Hae-Won Kim · Jonathan C. Knowles

Received: 12 March 2014 / Accepted: 20 October 2014 / Published online: 11 November 2014

Abstract Quaternary phosphate-based glasses in the P_2O_5–CaO–Na_2O–TiO_2 system with a fixed P_2O_5 and CaO content of 40 and 25 mol% respectively have been successfully synthesised via sol–gel method and bulk, transparent samples were obtained. The structure, elemental proportion, and thermal properties of stabilised sol–gel glasses have been characterised using X-ray diffraction (XRD), energy dispersive X-ray spectroscopy (EDX), ^{31}P nuclear magnetic resonance (^{31}P NMR), titanium K-edge X-ray absorption near-edge structure (XANES), fourier transform infrared (FTIR) spectroscopy, and differential thermal analysis (DTA). The XRD results confirmed the amorphous nature for all stabilized sol–gel derived glasses. The EDX result shows the relatively low loss of phosphorus during the sol–gel process and Ti K-edge XANES confirmed titanium in the glass structure is in mainly six-fold coordination environment. The ^{31}P NMR and FTIR results revealed that the glass structure consist of mainly Q^1 and Q^2 phosphate units and the Ti^{4+} cation was acting as a cross-linking between phosphate units. In addition DTA results confirmed a decrease in the glass transition and crystallisation temperature with increasing Na_2O content. Ion release studies also demonstrated a decrease in degradation rates with increasing TiO_2 content therefore supporting the use of these glasses for biomedical applications that require a degree of control over glass degradation. These sol–gel glasses also offer the potential to incorporate proactive molecules for drug delivery application due to the low synthesis temperature employed.

Keywords Sol–gel synthesis · Phosphate-based glass · NMR

F. Foroutan · G. Palmer · G. J. Owens · J. C. Knowles (✉)
Division of Biomaterials and Tissue Engineering/Eastman Dental Institute, University College London, 256 Gray's Inn Road, London WC1X 8LD, UK
e-mail: j.knowles@ucl.ac.uk

F. Foroutan · N. H. de Leeuw
Department of Chemistry/Faculty of Math and Physical Science, University College London, 20 Gordon Street, London WC1H 0AJ, UK

R. A. Martin
School of Engineering and Applied Sciences and Aston Research Centre for Healthy Ageing, Aston University, Birmingham B4 7ET, UK

H.-W. Kim · J. C. Knowles
Department of Nanobiomedical Science and BK21 PLUS NBM Global Research Center for Regenerative Medicine, Dankook University, Cheonan 330–714, Republic of Korea

H.-W. Kim
Institute of Tissue Regeneration Engineering (ITREN), Dankook University, Cheonan 330–714, Republic of Korea

H.-W. Kim
Department of Biomaterials Science, School of Dentistry, Dankook University, Cheonan 330–714, Republic of Korea

1 Introduction

Recently, interest in soft and hard tissue engineering to improve tissue regeneration has fuelled the need for novel biomaterials having specific bioactivity and controllable degradation rates [1]. Bioresorbable materials can be resorbed in the body and replaced by bone and tissue cells. In comparison with metallic implants which may exhibit complications such as tissue irritation and inflammation that may require secondary surgery to remove the implant;

resorbable materials offer a potential solution to these problems by eliminating the need for follow up surgery to remove the implant. Phosphate-based glasses show great potential to act as a bioresorbable material for biomedical applications, since they show a controllable degradation rate [2]. Moreover the break-down components can be easily metabolised in the body and their solubility can be controlled by varying its chemical composition [3, 4]. In recent years, there has been several papers on improving the physical properties and chemical durability of the phosphate glasses by adding different metal oxides with high valency cations such as Ti^{4+}, Fe^{3+}, etc., because of the formation of relatively stable cross-linked bonds in the phosphate network [5, 6]. Quaternary phosphate-based glasses of the general formula P_2O_5–CaO–Na_2O–TiO_2 (PCNT) have been prepared via melt-quench methods for biomedical application purposes [7]. Work on related systems has also been undertaken. For example, Kasuga has synthesized glasses in the CaO–TiO_2–P_2O_5 system [8] with TiO_2 content up to 10 mol% and melt quenched invert glasses have also been prepared in the Na_2O–CaO–TiO_2–P_2O_5 system [9], but in this case with only 3 mol% TiO_2. However, both of these papers focused on converting these glasses to glass–ceramics. These glasses are bioresorbable with the release of Ca^{2+} ions that can stimulate gene up regulation and cell proliferation [10–13]. The TiO_2 content has been shown to be an efficient oxide to improve not only the chemical durability of the glass but also their mechanical properties that make these glasses more stable in water over long periods [14–16]. However, the high temperature nature of the melt-quench method restricts the type of molecule that can be incorporated [3, 7].

In the past decade, the sol–gel synthesis method has attracted increasing attention as a good alternative to the traditional melt-quench method. The low synthesis temperature of the sol–gel method leads to the opportunity to incorporate bioactive molecules into the glass for drug delivery applications, which can be homogeneously dispersed throughout the sol–gel derived glass during the synthesis procedure [17, 18]. The degradation rate for these glasses can be controlled according to the glass composition. In addition the biocompatibility of these glasses may also offer a significant advantage over the current polymer-based systems where their degradation can result in polymer fragments with heterogeneous chain-lengths that could lead to toxicity. However, to the date there have been no reports of sol–gel preparation of these quaternary phosphate-based glasses.

Here for the first time we report sol–gel preparation of quaternary P_2O_5–CaO–Na_2O–TiO_2 glass systems. The structure of these glass samples has been characterized using XRD, XANES, ^{31}P MAS-NMR, DTA, and FTIR spectroscopy. The elemental proportion measured by EDX and also the effect of substitution sodium for titanium on the structure has been studied.

2 Materials and methods

2.1 Materials

The following chemical precursors have been used without further purification; n-butyl phosphate (1:1 molar ratio of mono $OP(OH)_2(OBu^n)$ and di-butyl phosphate $OP(OH)(OBu^n)_2$, Alfa Aesar, 98 %), titanium isopropoxide ($Ti(OPr^i)_4$, Aldrich, 95 %), calcium methoxyethoxide (Ca-methoxyethoxide, ABCR, 20 % in methoxyethanol), sodium methoxide solution (NaOMe, Aldrich, 30 wt% in methanol), 2-methoxyethanol (MeO-EtOH, Aldrich, 99.8 %), and n-dimethyl formamide (n-DMF, Alfa-Aesar, 99.8 %).

2.2 Synthesis of the sol

The reaction was started by diluting n-butyl phosphate in MeO-EtOH at the molar ratio of 1:3 and allowing them to react for 10 min (the whole reaction being carried out in a dried vessel). Then $Ti(OPr^i)_4$ was added to the mixture while it was magnetically stirring. Following that after 1 h stirring Ca-methoxyethoxide was added dropwise into the vessel. Stirring was continued for about 1 h and then in the last stage the vessel was cooled down in an ice-bath before NaOMe and n-DMF were added to the solution. The sol–gel preparation is outlined by the flowchart in Fig. 1 Drying procedure.

For all samples the clear mixture was poured into a glass container and allowed to gel at room temperature. The mixtures turned to gel after about 3 min and were then aged for 3 days at room temperature. Following the drying stage, the temperature was increased to 60 °C and held for 7 days, and then to 120 °C for 4 days before drying at 170 °C for 2 days and 220 °C for 1 h to remove any remaining solvent and to obtain bulk, glassy-like samples (Fig. 2). Table 1 shows the effect of drying procedure in the PCNT glass samples.

2.3 Characterization

2.3.1 X-ray diffraction

The XRD was obtained by a Bruker-D8 Advance Diffractometer (Brüker, UK) on fine glass powders in flat plate geometry using Ni filtered Cu Kα radiation. Data was collected using a Lynx Eye detector with a step size of 0.02° over an angular range of $2\theta = 10$–100° and a count time of 12 s.

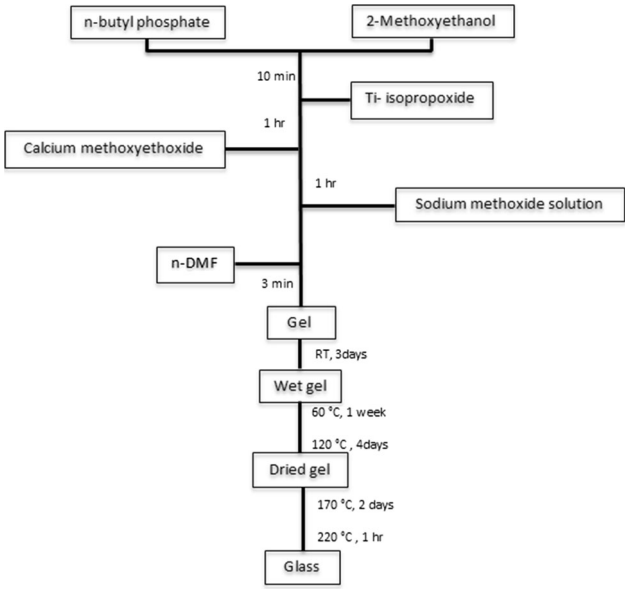

Fig. 1 Flow diagram of the quaternary PCNT sol–gel glasses

2.3.2 EDX analysis

Energy dispersive X-ray spectroscopy (EDX)- Inca 300 (Oxford instrument, UK) was used to determine the exact compositions of the prepared samples. Scanning electron microscopy (SEM)-XL30 (Philips, Netherland) was operated at 20 kV, spot size 5, and working distance of 10 mm to identify the particular elements and their relative proportions with EDX from the scanned area.

2.3.3 XANES study

Titanium K-edge X-ray absorption near-edge structure (XANES) data was collected using the micro-focus beam line I18 at the Diamond Light source, UK. Data were collected from 80 to 220 eV below and above the edge respectively to allow an accurate background subtraction and all measurements were made at room temperature.

2.3.4 MAS NMR

The solid state ^{31}P MAS-NMR spectrum was acquired on a Varian VNMRS-400 spectrometer and was referenced to the resonance of the secondary reference ammonium di-hyrogen phosphate ($NH_4H_2PO_4$) at 0.9 ppm (relative to 85 % H_3PO_4 solution at 0 ppm). The spectrum was recorded at 161.87 MHz for which glass powders were loaded into a 4 mm (rotor o.d.) magic angle spinning probe. The spectrum was obtained using direct excitation (with a 90° pulse) with a 60 s recycle delay at ambient probe temperature (~25 °C) at a sample spin rate of 10 kHz and between 20 and 88 repetitions were accumulated.

2.3.5 FT-IR spectroscopy

The FTIR spectrum of the glass powders was collected using a Perkin Elmer spectrometer 2000 (USA). Glass powder was scanned at room temperature in the absorbance mode in the range of 4,000–600 cm^{-1}. The obtained data was analysed by the software supplied by Perkin Elmer Co.

2.3.6 Thermal analysis

Differential thermal analysis of the glass powders was carried out on a Setaram Labsys™ TG–DTA-16 instrument with a heating rate of 20 °C min^{-1} from 20 to 1,000 °C in a Pt crucible and a purge gas of air. The data was base-line corrected using a blank run and glass transition (T_g) and crystallisation temperature (T_c) were measured.

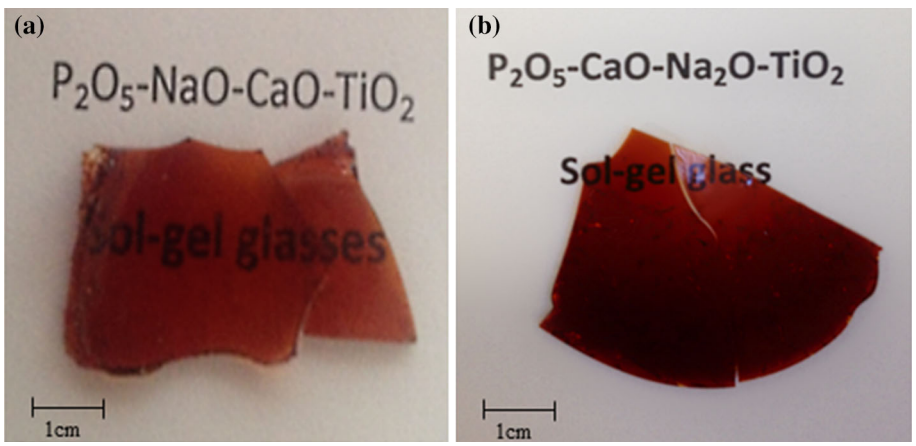

Fig. 2 Photographs of quaternary PCNT sol–gel glasses

Table 1 The effect of drying procedure in quaternary PCNT sol–gel glasses

Sample code	Sample	Gelation at room temperature	Transparency	Bulk sample
PCNT1	$P_{40}Ca_{25}Na_5Ti_{30}$	✓	✓	Few cracks
PCNT2	$P_{40}Ca_{25}Na_{10}Ti_{25}$	✓	✓	Few cracks
PCNT3	$P_{40}Ca_{25}Na_{15}Ti_{20}$	✓	✓	Heavily cracked

2.3.7 *Ion release study*

The obtained sol–gel glasses were ground to form microparticles using a Retsch MM301 milling machine operated at 10 Hz frequency (Retsch, Germany). The microparticles in the size range of 106–150 m were obtained by passing them through 150 and 106 m sieves (Endecotts ltd, UK) on a Fritsch Spartan sieve shaker (Fritsch GmbH, Germany). For the ion release study, 1 mg of each of the glass composition chosen were immersed in deionized water for 2 h. The resulting suspensions were centrifuged at 4,600 rpm for 6 min to separate the glass from the solution. The liquid phase was then extracted and the glass subsequently re-suspended in 10 mL dH-$_2$O for a further 4 h. This process was repeated to gain liquid samples following 24 and 48 h total immersion times. Calcium, phosphorous, sodium and titanium in solution were subsequently measured by ICP-MS using a Spectro Mass 2000 Analytical System calibrated across the predicted concentrations range 0–4,000 ppb by dilution of 100 ppm elemental standards. Calcium and titanium standards were obtained as part of a pre-made standard solution (Fluka) whereas phosphorous and sodium standards were created from analytical grade K_2HPO_4 (Sigma) and $NaNO_3$ (Sigma) salts respectively. Standards were first diluted in dH_2O to result in the desired concentration range. Both samples and standards were diluted in 1:1 in 4 % HNO_3 (Fluka) and analysed in reference to a blank (2 % HNO_3) solution under standard operating conditions (power: 1350 W; Coolant Flow: 15 L min^{-1}: Axillary Flow: 1 L min^{-1}). Results were expressed as cumulative ion release over the full period of the degradation study.

3 Results

3.1 X-ray diffraction

The XRD pattern was free from any detectable crystalline phase (Fig. 3) and a broad peak at 2θ values of around 20–40° was observed for all samples. These patterns confirmed the glassy nature of all samples.

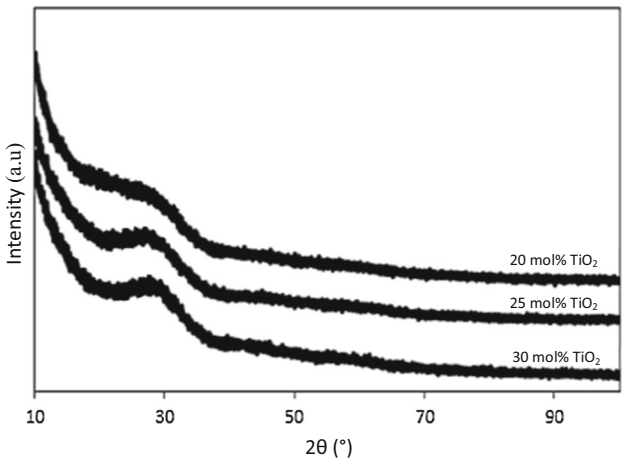

Fig. 3 XRD spectra of quaternary PCNT glasses

3.2 EDX analysis

The EDX results were reported in Table 2. The P_2O_5 content showed a reduction of around 4–5 mol% from the theoretical values, with a concomitant increase in the percentage content of the other oxides to compensate.

3.3 Ti K-edge XANES study

Figure 4 shows the Ti K-edge XANES data for the 20, 25, and 30 mol% TiO_2 doped phosphate glasses. The pre-edge data for the samples contain 20 and 25 mol% TiO_2 consist of two small peaks at 4,968 and 4,970 eV with normalized intensities of 0.06 and 0.12 respectively that show Ti occupying a six-fold coordination (TiO_6) environment [14]. However for the sample containing 30 mol% TiO_2 the first peak is broader and the intensity of the second peak at 4,970 eV raises to 0.27 suggestion that a small proportion of 4 or fivefold Ti may be present [19, 20].

3.4 Solid state ^{31}P MAS-NMR

With ^{31}P nucleus NMR analysis, there is the possibility to measure the relative quantities of the various Q^i species that comprise the glass structure. The PO_4^{3-} tetrahedron is the base component of the phosphate-based glasses. Phosphate tetrahedra are classified by the number of oxygen atoms they share with other phosphate tetrahedra and an oxygen atom shared in this way is referred to bridging oxygen (BO) thereafter. According to Abou Neel et al. [2], the different type of phosphate tetrahedra are labelled referring to the number of BOs and ranges from Q^0 (an isolated PO_4^{3-} tetrahedral) to Q^3 (share three covalently

Table 2 Intended compositions and compositions determined by EDX (in brackets). for stabilized sol–gel glasses

Sample code	P_2O_5 (mol%)	CaO (mol%)	Na_2O (mol%)	TiO_2 (mol%)
PCNT1	40 (36.2 ± 1.1)	25 (26.7 ± 0.7)	5 (6.3 ± 0.7)	30 (30.8 ± 0.8)
PCNT2	40 (35.8 ± 1.3)	25 (26.9 ± 0.8)	10 (11.6 ± 0.9)	25 (25.7 ± 0.8)
PCNT3	40 (35.6 ± 1.2)	25 (26.9 ± 0.8)	15 (16.4 ± 0.8)	20 (21.1 ± 0.7)

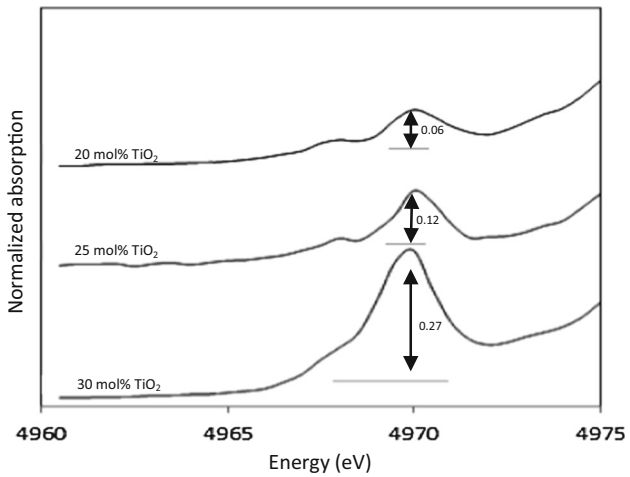

Fig. 4 Titanium K-edge X-ray absorption structure of stabilized sol–gel glasses

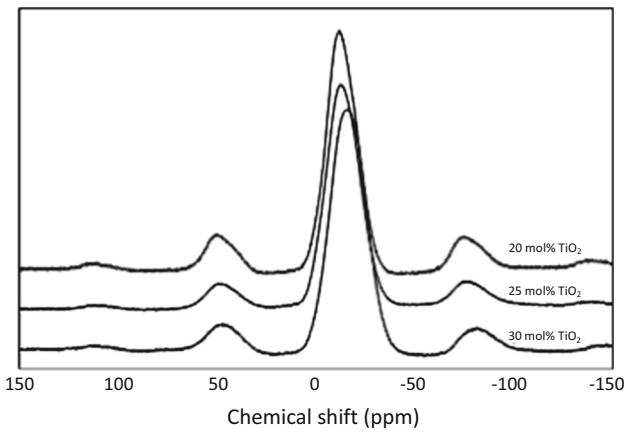

Fig. 5 The ^{31}P MAS NMR spectra of stabilized PCNT sol–gel

bonded BOs with neighbouring PO_4^{3-}). P_2O_5 consists of only Q^3 phosphate tetrahedra that form a three-dimensional network and the addition of metal oxides shows depolymerisation of phosphate network (Q^i species according to $Q^3 \rightarrow Q^2 \rightarrow Q^1 \rightarrow Q^0$ as the amount of modifying oxide increases) [21].

Figure 5 shows the ^{31}P-NMR spectrum of the glass powders. In order to obtain the relative abundance of the Q^i species, the intensities of the peaks were fitted by the DM-fit software and the isotropic chemical shifts and relative properties are reported in Table 3. The ^{31}P NMR results show broad peaks that contain Q^0, Q^1, and Q^2 phosphate groups.

The peaks between −1.2 and −0.2 ppm correspond to the presence of Q^0 units and peaks with the chemical shifts in the range of −10.3 to −10.0 ppm and −22.8 to −21.9 ppm are attributed to Q^1 and Q^2 species respectively [22]. While as suggested by Montagne et al. [23] the peaks with chemical shifts in the range between −14.8 and −14.1 ppm can be accounted for as due to the presence of an additional Q^1(Ti–O–P) peaks.

3.5 FTIR analysis

The FTIR spectra of the glass samples is presented in Fig. 6. The absorption bands can be assigned according to the previous FTIR studies on phosphate-based glasses [24–29]. The peak at 745 cm^{-1} can be assigned to symmetrical stretching υ_s (P–O–P) mode, while the peak at 900 and 1,175 cm^{-1} can be assigned to asymmetrical stretching υ_{as} (P–O–P) mode (Q^2 phosphate units). Also the peak at 970 and can be explained by Q^1 phosphate groups interacting with Ca^{2+}, and Na^+ cations. The peaks at 1,640, 3,015, and 3,400 cm^{-1} can be related to the absorbed moisture and the presence of hydroxyl groups in the glass samples. The main peaks and assignments are summarised in Table 4.

3.6 DTA analysis

Figure 7 shows the DTA graph of the 5–15 mol% Na_2O sol–gel glasses. From the DTA graphs, as expected, the T_g (a measure of the bulk properties of the glass) increases with increasing the TiO_2 content, rising from 485 to 573 °C. The first observed exothermic shifts are attributed to the crystallization temperatures which show two crystallization events. As shown the glasses containing 5 mol% Na_2O, had two crystallization phases at around 697 and 740 °C. While by increasing the amount of sodium to 10 mol%, the crystalline phases appeared at lower temperature of 638 and 664 °C respectively. The addition of 15 mol% Na_2O, results in a further decrease in crystallisation temperature to 594 and 645 °C.

Table 3 The 31P MAS NMR peak parameters of stabilized PCNT sol–gel glasses

Glass code	Sample	Position (ppm) (±0.2)	Q^i species	Line width (ppm) (±0.2)	Abundance (%) (±1.0)
PCNT1	$P_{40}Ca_{25}Na_5Ti_{30}$	−1.2	0	7.7	2.0
		−10.3	1	9.8	29.1
		−14.8	1	9.9	40.8
		−22.8	2	11.8	28.1
PCNT2	$P_{40}Ca_{25}Na_{10}Ti_{25}$	−0.8	0	7.4	3.4
		−10.1	1	9.7	37.4
		−14.4	1	9.9	35.7
		−22.5	2	11.7	23.5
PCNT3	$P_{40}Ca_{25}Na_{15}Ti_{20}$	−0.2	0	6.8	4.1
		−10.0	1	9.5	41.3
		−14.1	1	9.6	33.2
		−21.9	2	11.2	21.4

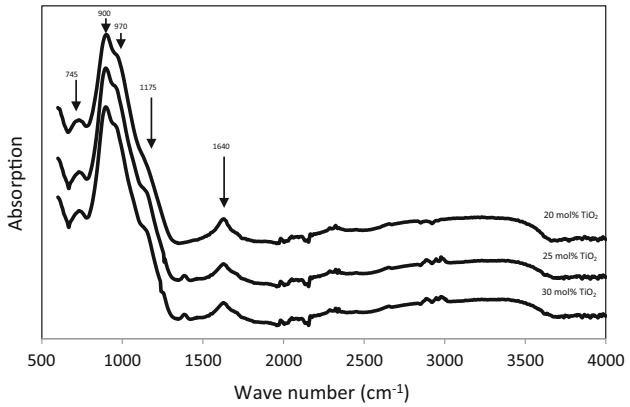

Fig. 6 Infra-red spectra from the stabilized PCNT sol–gel glasses

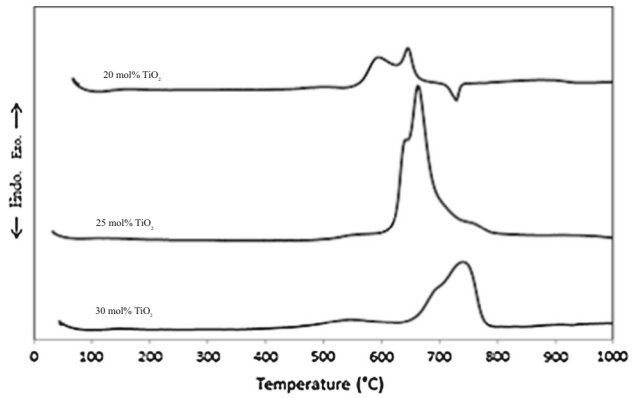

Fig. 7 Differential thermal analysis traces of the stabilized PCNT sol–gel glasses

Table 4 Infrared band assignment for stabilised PCNT sol–gel glasses (υ, stretching; s, symmetric; as, asymmetric)

Wave number (cm^{-1})	Assignment	Associated Q^i (where applicable)
745	υ_s (P–O–P)	
900	υ_{as} (P–O–P)	Q^2
970	υ_s (PO_3)	Q^1
1,175	υ_{as} (PO_2)	Q^2

3.7 Ion release study

The concentration of calcium, phosphorous, sodium and titanium released into solution are presented in Fig. 8 for each of the chosen glass compositions. As expected, glasses with the lowest Ti content exhibited the highest degree of ion release. Likewise, higher Ti content glasses released the least amount of network-forming elements into solution.

4 Discussion

In the present study, it was possible to synthesize PCNT glass systems with high TiO_2 content via the sol–gel method. While, incorporating a high percentage of titanium into phosphate network is non-trivial via melt-quench method and according to the literature the maximum percentage may reach to 15 mol% in quaternary phosphate-based glasses [7]. The XRD results revealed the glassy nature for all samples and the EDX result shows relatively low loss of phosphorus (calculated as mol% P_2O_5) during the sol–gel process. This loss is to be expected due to the relative volatility of both the precursor used and the end product from that precursor. The Ti K-edge XANES data revealed that the structure of the stabilized sol–gel glasses contain 20 and 25 mol% Ti consist of mainly TiO_6 octahedra. Data comparison of the sol–gel and the melt-quenched glasses, shows that they have a similarity in the position and intensity of the pre-edge peaks [14]. While, for the sample

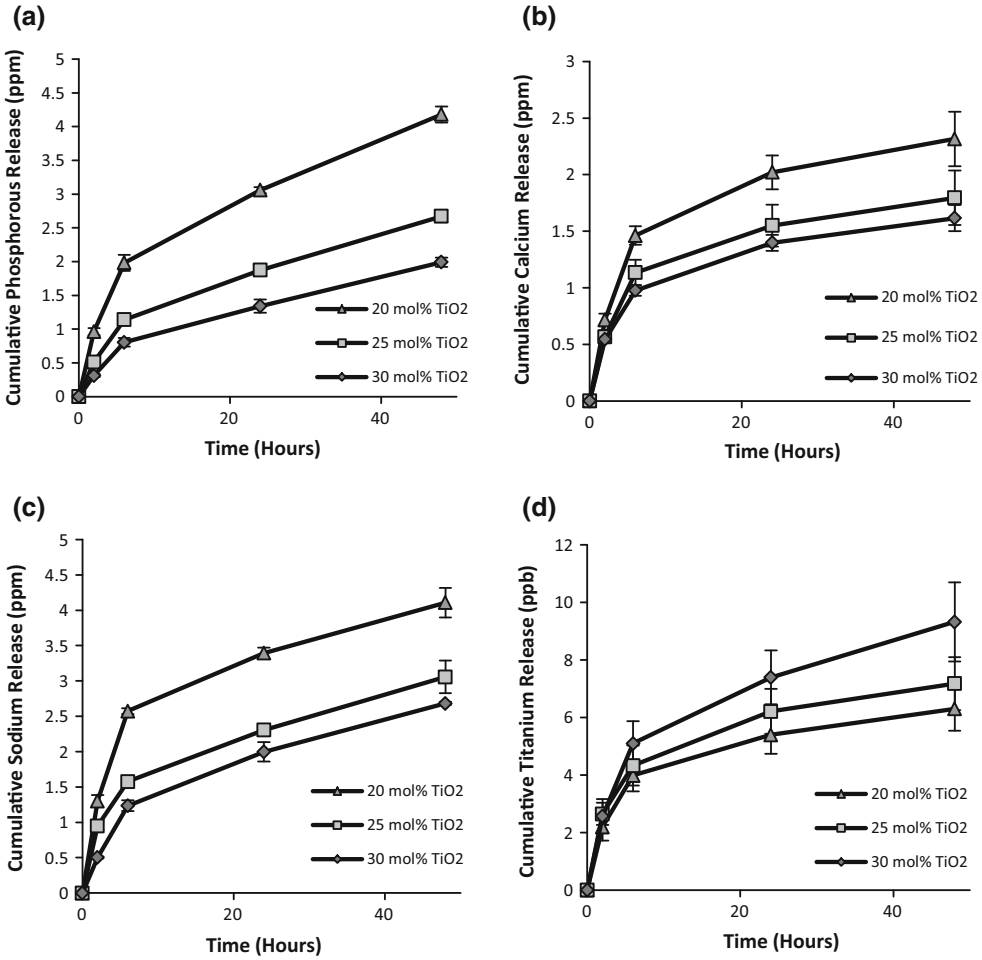

Fig. 8 Cumulative release of **a** phosphorous, **b** calcium, **c** sodium, and **d** titanium in the solution as a function of time for the investigated sol–gel glasses

containing 30 mol% TiO_2, appears to be small fraction of 4 or fivefold coordinated Ti that maybe related to the unreacted titanium precursor. The ^{31}P NMR spectra show that the chemical shifts are sensitive to the glass composition and with increasing the amount of Na_2O, each peak becomes less shielded (less negative chemical shift) with decreasing polymerisation of the phosphate network (fewer bridging oxygens per tetrahedron) [30]. The Ti^{4+} units acting as a cross-linking between phosphate units, thereby impeding crystallisation as a chain hydration and subsequent chain dissolution compared to Na^+ cations. In the FTIR spectra of the stabilized sol–gel glasses, the peak at 900 and 970 cm^{-1} can be attributed to Q^2 and Q^1 phosphate groups respectively. The peak at 1,175 cm^{-1} can be explained by Q^2 phosphate groups with a stronger peak with higher amount of titanium. This finding represents a depolymerization in the phosphate connectivity with increasing sodium as confirmed by the ^{31}P NMR data. The DTA results show increases in the glass transition temperature by increasing the amount of titanium due to the formation of P–O–Ti bonds that forms cross-linking between non-bridging of the two different chains (as observed in NMR and FT-IR results). These interconnections within the structural network can strengthen the glass structure and reduce the degradation rate of these glasses [31].

According to the previous studies on quaternary PCNT melt-quench glasses, higher degradation rates are expected for samples containing larger concentrations of sodium; this can be reduced by substituting sodium for titanium [7, 10]. As was confirmed within the present work, degradation rates of sol–gel glasses can be controlled by changing the composition of the glass in this same way; this makes them a very good choice for their biomedical application in the future. In addition, the low synthesis temperature via sol–gel method allows us to incorporate active biological ingredients like proteins and drug molecules into the glass structure and applying them as a carrier for drug delivery system.

Moreover, since the process starts with the liquid form of precursors, producing nano/micro meter sized particles for biomedical application would be much easier in comparison with the melt-quench method.

5 Conclusion

In this study for the first time quaternary glasses in the system $(P_2O_5)_{0.4}$–$(CaO)_{0.25}$–$(Na_2O)_X$–$(TiO_2)_{(0.35-X)}$ (x = 0.05, 0.10, and 0.15) have been successfully synthesized via sol–gel method. The amorphous pattern and glassy nature were confirmed by X-ray diffraction and EDX results revealed loss of phosphorus during the sol–gel process is relatively low. The ^{31}P NMR, FTIR, and ion release data show that TiO_2 improve cross-linking of the phosphate units by formation of Q^1(Ti) species that can decrease their solubility for biomedical applications. The XANES study results confirm that the titanium in the glass structure consist of mainly TiO_6 octahedra and differential thermal analysis shows that the glass transition temperature decreased by substituting sodium for titanium. Future work will be undertaken on production of nano/micro size glass beads for their potential drug delivery application.

Acknowledgments The authors would like to thank to EPSRC NMR Service at Chemistry Department- Durham University for the MAS NMR measurement and Diamond Light Source for the XANES measurement. This work was supported by the UCL Industrial Doctorate Centre in Molecular Modelling & Materials Science and in part (JCK & HWK) by National Research Centers Program (2009-0093829) through the National Research Foundation (NRF), Republic of Korea.

References

1. Hench LL, Polak JM (2002) Third-generation biomedical materials. Science 295: 1014-+
2. Abou Neel EA, Pickup DM, Valappil SP, Newport RJ, Knowles JC (2009) Bioactive functional materials: a perspective on phosphate-based glasses. J Mater Chem 19:690–701
3. Knowles JC (2003) Phosphate based glasses for biomedical applications. J Mater Chem 13:2395–2401
4. Franks K, Abrahams I, Georgiou G, Knowles JC (2001) Investigation of thermal parameters and crystallisation in a ternary CaO–Na(2)O–P(2)O(5)-based glass system. Biomaterials 22:497–501
5. Minami T, Mackenzie JD (1977) Thermal-expansion and chemical durability of phosphate glasses. J Am Ceram Soc 60:232–235
6. Lakhkar N, AbouNeel EA, Salih V, Knowles JC (2011) Titanium and strontium-doped phosphate glasses as vehicles for strontium ion delivery to cells. J Biomater Appl 25:877–893
7. Kiani A, Lakhkar NJ, Salih V, Smith ME, Hanna JV, Newport RJ et al (2012) Titanium-containing bioactive phosphate glasses. Philos T R Soc A 370:1352–1375
8. Kasuga T (2005) Bioactive calcium pyrophosphate glasses and glass-ceramics. Acta Biomater 1:55–64
9. Kasuga T, Sawada M, Nogami M, Abe Y (1999) Bioactive ceramics prepared by sintering and crystallization of calcium phosphate invert glasses. Biomaterials 20:1415–1420
10. Navarro M, Ginebra MP, Planell JA (2003) Cellular response to calcium phosphate glasses with controlled solubility. J Biomed Mater Res, Part A 67A:1009–1015
11. Navarro M, Clement J, Ginebra MP, Martinez S, Avila G, Planell JA (2002) Improvement of the stability and mechanical properties of resorbable phosphate glasses by the addition of TiO_2. Key Eng Mat 218–2:275–278
12. Lakhkar NJ, Park JH, Mordan NJ, Salih V, Wall IB, Kim HW et al (2012) Titanium phosphate glass microspheres for bone tissue engineering. Acta Biomater 8:4181–4190
13. Vitale-Brovarone C, Ciapetti G, Leonardi E, Baldini N, Bretcanu O, Verne E et al (2011) Resorbable glass-ceramic phosphate-based scaffolds for bone tissue engineering: synthesis, properties, and in vitro effects on human marrow stromal cells. J Biomater Appl 26:465–489
14. Pickup DM, Abou Neel EA, Moss RM, Wetherall KM, Guerry P, Smith ME et al (2008) TiK-edge XANES study of the local environment of titanium in bioresorbable TiO(2)–CaO–Na(2)O–P(2)O(5) glasses. J Mater Sci-Mater Med; 19:1681–1685
15. Brow RK, Tallant DR, Warren WL, McIntyre A, Day DE (1997) Spectroscopic studies of the structure of titanophosphate and calcium titanophosphate glasses. Phys Chem Glasses 38: 300–306
16. Navarro M, Ginebra MP, Clement J, Martinez S, Avila G, Planell JA (2003) Physicochemical degradation of titania-stabilized soluble phosphate glasses for medical applications. J Am Ceram Soc 86:1345–1352
17. Pickup DM, Newport RJ, Knowles JC (2012) Sol–gel phosphate-based glass for drug delivery applications. J Biomater Appl 26:613–622
18. Carta D, Pickup DM, Knowles JC, Smith ME, Newport RJ (2005) Sol–gel synthesis of the P(2)O(5)–CaO–Na(2)O–SiO(2) system as a novel bioresorbable glass. J Mater Chem 15:2134–2140
19. Farges F (1996) Coordination of Ti in crystalline and glassy fresnoites: a high-resolution XANES spectroscopy study at the Ti K-edge. J Non-Cryst Solids 204:53–64
20. Farges F, Brown GE, Rehr JJ (1997) Ti K-edge XANES studies of oxides: theory vs. experiment. J Phys IV 7:191–193
21. Kirkpatrick RJ, Brow RK (1995) Nuclear-magnetic-resonance investigation of the structures of phosphate and phosphate-containing glasses: a review. Solid State Nucl Magn Reson 5:9–21
22. Lee IH, Foroutan F, Lakhkar NJ, Gong MS, Knowles JC (2013) Sol–gel synthesis and structural characterization of P2O5–CaO–Na2O glasses. Phys Chem Glasses-Eur J Glass Sci Technol Part B 54:115–120
23. Montagne L, Daviero S, Palavit G (2003) Glass network evolution with Bi3 +/Ti4 + substitution in phosphate glasses formulated with a constant oxygen/phosphorus ratio. EXAFS, XANES, and P-31 double quantum MAS NMR. Chem Mater 15:4709–4716
24. Baia L, Muresan D, Baia M, Popp J, Simon S (2007) Structural properties of silver nanoclusters-phosphate glass composites. Vib Spectrosc 43:313–318

25. Byun JO, Kim BH, Hong KS, Jung HJ, Lee SW, Izyneev AA (1995) Properties and structure of Ro-Na2o–Al2o3–P2o5 (R = Mg, Ca, Sr, Ba) glasses. J Non-Cryst Solids 190:288–295
26. Ilieva D, Jivov B, Kovacheva D, Tsacheva T, Dimitriev Y, Bogachev G et al (2001) FT-IR and Raman spectra of Gd phosphate crystals and glasses. J Non-Cryst Solids 293:562–568
27. Moustafa YM, El-Egili K (1998) Infrared spectra of sodium phosphate glasses. J Non-Cryst Solids 240:144–153
28. Brauer DS, Karpukhina N, Law RV, Hill RG (2010) Effect of TiO_2 addition on structure, solubility and crystallisation of phosphate invert glasses for biomedical applications. J Non-Cryst Solids 356:2626–2633
29. Abou Neel EA, Chrzanowski W, Pickup DM, O'Dell LA, Mordan NJ, Newport RJ et al (2009) Structure and properties of strontium-doped phosphate-based glasses. J R Soc Interface 6:435–446
30. Brow RK, Kirkpatrick RJ, Turner GL (1990) The short-range structure of sodium-phosphate glasses.1. Mas Nmr-Studies. J Non-Cryst Solids 16:39–45
31. Abou Neel EA, Chrzanowski W, Valappil SP, O'Dell LA, Pickup DM, Smith ME et al (2009) Doping of a high calcium oxide metaphosphate glass with titanium dioxide. J Non-Cryst Solids 355:991–1000